RESEARCH ARTICLE

[18F]DPA-714 PET Imaging in the Presurgical Evaluation of Patients With Drug-Resistant Focal Epilepsy

Margaux Cheval, MD, Sebastian Rodrigo, MD, PhD, Delphine Taussig, MD, PhD, Fabien Caillé, PhD, Ana Maria Petrescu, MD, Michel Bottlaender, MD, Nicolas Tournier, PharmD, PhD, Florent L. Besson, MD, PhD, Claire Leroy, PhD, and Viviane Bouilleret, MD, PhD

Correspondence
Dr. Cheval
margaux.cheval@aphp.fr

Neurology® 2023;101:e1893-e1904. doi:10.1212/WNL.0000000000207811

Abstract

Background and Objectives

Translocator protein 18 kDa (TSPO) PET imaging is used to monitor glial activation. Recent studies have proposed TSPO PET as a marker of the epileptogenic zone (EZ) in drug-resistant focal epilepsy (DRFE). This study aims to assess the contributions of TSPO imaging using [18F]DPA-714 PET and [18F]FDG PET for localizing the EZ during presurgical assessment of DRFE, when phase 1 presurgical assessment does not provide enough information.

Methods

We compared [18F]FDG and [18F]DPA-714 PET images of 23 patients who had undergone a phase 1 presurgical assessment, using qualitative visual analysis and quantitative analysis, at both the voxel and the regional levels. PET abnormalities (increase in binding for [18F]DPA-714 vs decrease in binding for [18F]FDG) were compared with clinical hypotheses concerning the localization of the EZ based on phase 1 presurgical assessment. The additional value of [18F]DPA-714 PET imaging to [18F]FDG for refining the localization of the EZ was assessed. To strengthen the visual analysis, [18F]DPA-714 PET imaging was also reviewed by 2 experienced clinicians blind to the EZ location.

Results

The study included 23 patients. Visual analysis of [18F]DPA-714 PET was significantly more accurate than [18F]FDG PET to both, show anomalies (95.7% vs 56.5%, $p = 0.022$), and provide additional information to refine the EZ localization (65.2% vs 17.4%, $p = 0.019$). All 10 patients with normal [18F]FDG PET had anomalies when using [18F]DPA-714 PET. The additional value of [18F]DPA-714 PET seemed to be greater in patients with normal brain MRI or with neocortical EZ (especially if insula is involved). Regional analysis of [18F]DPA-714 and [18F]FDG PET provided similar results. However, using voxel-wise analysis, [18F]DPA-714 was more effective than [18F]FDG for unveiling clusters whose localization was more often consistent with the EZ hypothesis (87.0% vs 39.1%, $p = 0.019$). Nonrelevant bindings were seen in 14 of 23 patients in visual analysis and 9 patients of 23 patients in voxel-wise analysis.

Discussion

[18F]DPA-714 PET imaging provides valuable information for presurgical assessments of patients with DRFE. TSPO PET could become an additional tool to help to the localization of the EZ, especially in patients with negative [18F]FDG PET.

Trial Registration Information

Eudract 2017-003381-27. Inclusion of the first patient: September 24, 2018.

Classification of Evidence

This study provides Class IV evidence on the utility of [18F]DPA-714 PET compared with [18F]FDG PET in identifying the epileptic zone in patients undergoing phase 1 presurgical evaluation for intractable epilepsy.

MORE ONLINE

Class of Evidence
Criteria for rating therapeutic and diagnostic studies
NPub.org/coe

From the Université Paris-Saclay (M.C., C.L., M.B., N.T.); BioMAPS (S.R., F.C., F.L.B.); Bicetre University Hospital (D.T., A.M.P.), Paris; and Imagerie Moléculaire In Vivo (V.B.), SHFJ, CEA, Orsay, France.

Go to Neurology.org/N for full disclosures. Funding information and disclosures deemed relevant by the authors, if any, are provided at the end of the article.

Glossay

[^{18}F]**DPA-714** = [N,N-diethyl-2-(2-(4-(2[^{18}F]-fluoroethoxy)phenyl)5,7dimethylpyrazolo [1,5a]pyrimidin-3-yl)acetamide; [^{18}F]**FDG** = [^{18}F]-fluoro-deoxyglucose; **AI** = asymmetry index; **ASM** = antiseizure medication; **DRFE** = drug-resistant focal epilepsy; **DVR** = distribution volume ratio; **EZ** = epileptogenic zone; **FWHM** = full width at half maximum; **HAB** = high-affinity binder; **LAB** = low-affinity binder; **MAB** = mild-affinity binder; **MNI** = Montreal Neurological Institute; **MTLE** = mesial temporal lobe epilepsy; **ROI** = region of interest; **SPM** = statistical parametric mapping; **SUV** = standardized uptake value; **SVCA** = supervised cluster analysis; **TSPO** = translocator protein 18 kDa.

Introduction

Surgery is the only curative treatment for one-third of patients with drug-resistant focal epilepsy (DRFE).[1] Precise localization of the epileptogenic zone (EZ) is crucial for the success of surgery, but EZ localization remains challenging. Currently, the phase 1 presurgical assessment of DRFE integrates data from both interictal and ictal video EEG recordings, morphologic data from MRI, and metabolic data from [^{18}F]FDG PET.[2,3] These investigations are used by epileptologists to make hypotheses about the EZ localization. In 60% of cases, phase 1 presurgical assessment provides sufficiently accurate information to suggest immediate surgery. However, in 40% of the cases, it does not provide enough information, especially when MRI or [^{18}F]FDG PET is negative or does not precisely delimit the EZ. [^{18}F]FDG PET plays a crucial role in the EZ delimitation, especially in patients with normal MRI, and thus is a determining factor in the postsurgical prognosis.[4,5] So far, [^{18}F]FDG is the only PET radiopharmaceutical validated as a useful tool in the presurgical assessment of DRFE[6] with a sensitivity range of 70%–90% in patients with mesial temporal lobe epilepsy (MTLE).[7] Considering all locations and etiologies of DRFE, the localizing value of [^{18}F]FDG PET declines to a range of 40%–60%, with lower sensitivity when MRI is negative.[6] This underlines the clinical interest of finding alternative tracers to improve accurate localization of the EZ.

[^{18}F]DPA-714 has been proposed as a new PET radiotracer in epilepsy.[8] [^{18}F]DPA-714 binds to the translocator protein 18 kDa (TSPO), found in activated glial cells and astrocytes during inflammatory process, as identified in the EZ.[9-11] Several PET studies using specific TSPO-PET radiotracers have been performed in epilepsy, reporting an increase in the PET signal homolateral to the EZ in mesial temporal epilepsy as in other focal epilepsies.[12-18] However, its comparison with the currently validated [^{18}F]FDG PET has not been studied yet.

Several TSPO ligands were developed since 1980. The first generation of radiotracers ([^{11}C]PK11195) had several limitations: low signal-to-noise ratio due to the important aspecific binding and variable pharmacokinetics.[19] These limitations prompted the development of second-generation TSPO ligands, representing more than 50 candidates in preclinical studies (including ligands used in human studies as [^{18}F]PBR111, [^{11}C]PBR28, [^{11}C]DPA-713, [^{18}F]DPA-714) with better affinity and signal-to-noise ratio.[19] However, it introduced a new challenge as their affinity is influenced by a polymorphism (rs6971), defining 3 groups of binders (low-affinity binder [LAB, 9%], high-affinity binder [HAB, 49%], mixed-affinity binder [MAB, 42%]), depending on the number of alleles involved.[20] Human and experimental studies have shown that [^{18}F]DPA-714 has a more specific binding than its competitors and a better pharmacokinetic brain availability.[11,21-23] These results are promising for the study of pathophysiologic mechanisms and therapy of many brain diseases.

In this study, we aimed to assess whether [^{18}F]DPA-714 PET brings additional information compared with those of [^{18}F]FDG PET, for the EZ localization, in patients with DRFE for whom the phase 1 presurgical assessment was not sufficiently conclusive.

Methods

Population Selection

Patients with DRFE were recruited from the epileptology unit of a tertiary university hospital. All the included patients underwent a phase 1 presurgical assessment to establish a hypothesis on the EZ localization but with insufficient delineation for immediate surgery. Genomic DNA from blood samples was used to genotype the rs6971 polymorphism of the TSPO gene and to stratify all subjects' binders status. In addition to the standard exclusion criteria for PET and MRI, patients with LAB rs6971 polymorphism were excluded as well as patients with extensive brain lesions (large post-traumatic lesions, vascular lesions, tumors). They were all on the same antiseizure medication for at least 4 months. Both PET acquisitions were performed without medication withdrawal.

Standard Protocol Approvals, Registrations, and Patient Consents

The study (Eudract 2017-003381-27) was approved by the local ethics committee "CPP Ile-de-France 1" (RCB 2017-003381-27). All the patients signed an informed consent form for the PET examination and the use of medical data.

Demographic, Clinical, EEG, and Morphologic Imaging Data Collection

Demographic and clinical history data were collected by the physicians specialized in epilepsy surgery. MRI of the brain was reviewed by a neuroradiologist team. The hypothesis on the EZ localization was retained after concertation, during the epilepsy expert team meeting, based on the phase 1 presurgical assessment, including ictal video EEG. The time of last seizure before each PET was collected.

PET Acquisition, Reconstruction, and Image Processing

For each patient, the 2 PET acquisitions ([^{18}F]FDG PET first) were performed within a period of 1 year. All the [^{18}F]FDG PET data were acquired on the same PET/CT system (Siemens) according to the international clinical reference standards. All the [^{18}F]FDG PET data were corrected for attenuation (CT-based). For the voxel-wise and region-of-interest analysis, we used a database of 30 [^{18}F]FDG PET from healthy volunteers, acquired with the same camera, as previously reported.[24] Each [^{18}F]FDG PET image was processed according to standard care to obtain the standardized uptake value (SUV) parametric maps.

[^{18}F]DPA-714 PET data were acquired using a PET-MRI system (GE Healthcare) following the previously published standardized procedure.[10] In brief, bolus [^{18}F]DPA-714 (195.3 ± 19.7 MBq) was IV injected followed by 90-minute dynamic acquisition. [^{18}F]DPA-714 PET was corrected for attenuation (MR-based zero-echo-time method).[25] For the voxel-wise and region-of-interest analysis, a database of [^{18}F]DPA-714 PET images was used, obtained from 11 healthy volunteers acquired on the same PET-MR system and using the same protocol as the patients (mean age 41.27 ± 13.50 years, 63.64% [7] male and 36.36% [4] female, 54.54% [6] HAB and 45.46% [5] MAB). Supervised cluster analysis (SVCA) technique was performed to extract voxels used as a pseudoreference region.[26-28] Thereafter, parametric images of distribution volume ratio (DVR) values were calculated using TURKU software on a VOI basis, using the Logan reference plot throughout the imaging time with pseudoreference tissue obtained from SVCA, according to a previous study.[29] Based on FreeSurfer MRI anatomical T1 segmentation, a mask excluding extracerebral tissues was applied. The images were smoothed with a Gaussian filter (full width at half maximum [FWHM] = 8 mm).

Visual Analysis

SUV-normalized [^{18}F]FDG PET images and parametric [^{18}F]DPA-714 DVR images, coregistered on anatomical T1, were displayed in the patient's own space, using viewer from FreeSurfer software (Freeview), with the Jet color scale ([^{18}F]FDG contrast setting ~1,494–18,342; [^{18}F]DPA-714 ~0.67–1.39). Observers were first trained to read the images of the healthy control data set. The analysis has been performed blinded (S.R. and F.L.B.) and unblinded (M.C. and V.B.) of the clinical data. When the 2 observers' decisions diverged, the case was reviewed together to provide a joined analysis. Observers were first trained to read the images of the healthy control data set.

Region-of-Interest Analysis and Asymmetry Index

We performed a quantitative analysis comparing PET values extracted from regions of interest (ROI) of each patient to those from the database of healthy controls (for demographic data, see above and below). [^{18}F]FDG and [^{18}F]DPA PET uptake values were extracted from PET images normalized in a common standardized stereotactic space, the Montreal Neurological Institute (MNI) space using SPM12 software (statistical parametric mapping). A total of 62 ROI were defined using the Hammers PET atlas[30] intersected with gray matter segmentation to exclude white matter considered irrelevant for changes in [^{18}F]FDG or [^{18}F]DPA-714 uptake values. [^{18}F]FDG SUV and [^{18}F]DPA-714 DVR values for each of the 62 ROI were obtained. In controls and for both PET examinations, we calculated the 95% CI of the SUV or DVR values for each ROI. We considered that the radiotracer fixation was increased for [^{18}F]DPA-714 in a ROI if the DVR value of the patient was above the upper limit of the 95% CI of controls. In opposite, we considered that the metabolism was decreased for [^{18}F]FDG, if the patient's SUV value was lower than the lower limit of the 95% CI of controls.

The asymmetry index (AI) of DVR and SUV values between the right and left cortical gray matter regions (200% × [left – right]/[left + right]) was also calculated. AIs for each ROI were compared with the 95% CI of AIs in the corresponding ROIs of healthy controls.

Voxel-Wise Analysis

A voxel-wise analysis was performed comparing each patient's PET to the healthy control database, using SPM12 software. In addition to the [^{18}F]FDG PET images of the patients, 30 [^{18}F]FDG PET images of controls (mean age 36.65 ± 11.78 years) were normalized to MNI space, using the template included in SPM12 and smoothed with a Gaussian filter (FWHM = 8). To normalize the [^{18}F]DPA-714 PET images, a template from the 11 healthy controls was generated. Parametric DVR [^{18}F]DPA-714 images of patients and healthy controls were normalized in the MNI space using our template and smoothed with a Gaussian filter (FWHM = 8). The voxel-wise analysis generates parametric statistical maps, highlighting significant differences in brain regions for each patient (2-sample *t* test). We included age, sex, and, genotype for [^{18}F]DPA-714 as covariables in the statistical design matrix. Statistical maps were displayed using a *p* value between <0.001 and <0.005 (uncorrected) and a minimal cluster size (k) = 50 contiguous voxels.

Collected Variables to Assess the Performance of Both PET Examinations for All 3 Analysis

To assess the performance of the [^{18}F]DPA-714 and [^{18}F]FDG PET examinations using the 3 analysis methods, we collected the following variables: (1) the sensitivity

(presence of an anomaly—yes/no; the intensity of anomaly [visually assessed]—none/mild/intense), (2) its accuracy to localize the EZ (topography matching the EZ hypothesis localization—no/partially/totally; topography providing new information to refine the EZ hypothesis—yes/no), and (3) we investigate the possibility that anomalies present with [^{18}F]FDG PET were not seen in [^{18}F]DPA-714 PET and vice versa. We also studied the presence of nonrelevant binding on [^{18}F]DPA-714 PET images. Each of these end points was assessed based on the hypothesis on the EZ localization.

Statistical Analysis

To compare the performance of the 2 examinations on the specified criteria, we used McNemar tests for the nonordinal categorical variables and Wilcoxon signed-rank tests for the ordinal categorical variables. We performed a correction for multiple testing using the Benjamini-Hochberg method. Subgroup analysis was performed to determine whether [^{18}F]DPA-714 PET performance was superior in some categories of patients, depending on the seizure frequency, the presence of a lesion on MRI, or the type of epilepsy (temporal mesial or neocortical). Owing to the exploratory purpose of this analysis and ROI analysis, no correction for multiple testing was done. To determine the interobserver agreement in visual analysis, we calculated Cohen κ coefficients for dichotomous variables and intraclass correlation coefficients (2-way mixed effects model, type 3) for ordinal categorical variables. All tests were 2-sided, and statistical significance was defined as $p < 0.05$. Statistical analysis was performed using R 4.1.2.

Data Availability

The data that support the findings of this study are available on request from the corresponding author. The data are not publicly available due to privacy or ethical restrictions. Our database is currently being converted to BIDS.

Results

Study Population

Among the 29 patients retained to participate in the study, 6 were excluded: 3 were LAB, 1 declined to participate before the [^{18}F]DPA-714 PET, 1 had a large intracerebral hemorrhage discovered during the [^{18}F]DPA-714 PET, and for 1 patient, an error occurred during the [^{18}F]DPA-714 PET image processing. Twenty-three patients were selected for PET data analysis. The median age at the time of the [^{18}F]DPA-714 PET was 31 years [Q1; Q3: 20; 35]. Twelve (52.2%) patients were male. Regarding the rs6971 polymorphism, 13 (56.5%) were HAB and 10 (43.5%) were MAB. The median age at the onset of epilepsy was 15 years [11; 20.5], and the median disease duration was 12 years [5; 19]. The median time from last seizure for each of the PET examinations was 4 days [1; 5.75]. None reported a seizure during PET acquisition. Regarding seizure frequency, 5 (21.7%) patients had daily seizures, 5 (21.7%) weekly seizures, and 13 (56.5%) monthly seizures. Based on clinical, EEG, and MRI data, 5 (21.7%) patients had MTLE and 18 (78.3%) had neocortical epilepsy. MRI of the brain was normal for 15 (65.2%) patients (for all the patients with MTLE and 10 (55.6%) patients with neocortical epilepsy). Table 1 presents the detailed characteristics of each patient.

Visual Analysis

In [^{18}F]DPA-714, the anomalies identified are the areas of increase of tracer fixation, whereas in [^{18}F]FDG, it is the area of decrease of tracer fixation. The agreement between the 2 observers varied from perfect to substantial agreement (eTable 1, links.lww.com/WNL/D114), and no difference was found between the observers who were blinded and unblinded to clinical data. Using [^{18}F]DPA-714 PET, anomalies detection was improved compared with the use of [^{18}F]FDG PET (95.7% vs 56.5%, $p = 0.022$, Table 2) and was more likely to provide new information to refine the EZ localization (65.2% vs 17.4%, $p = 0.019$). We were unable to identify any statistical differences in consistency with the hypothesis on the EZ. For 21 (91.3%) patients, [^{18}F]DPA-714 PET revealed anomalies that were not detected by [^{18}F]FDG PET. All patients with [^{18}F]FDG PET hypometabolism (n = 13) also displayed [^{18}F]DPA-714 PET anomalies, but for 4 of them, it was less extensive with [^{18}F]DPA-714 PET. Over the 10 patients with normal [^{18}F]FDG PET, all had anomalies on [^{18}F]DPA-714 PET images. As shown in Figure 1, [^{18}F]DPA-714 PET helps to detect anomalies that were subtle or not seen on [^{18}F]FDG PET. However, nonrelevant bindings were found in 14 patients (60.9%).

Data from the subgroup analysis are available in eTables 2–4 (links.lww.com/WNL/D114). Subgroup analysis suggests that the additional value of [^{18}F]DPA-714 PET compared with [^{18}F]FDG PET seems to be greater in patients with normal brain MRI or with neocortical EZ than in patients with abnormal MRI or mesial temporal EZ. We did not find a conclusive difference in the additional value of [^{18}F]DPA-714 PET compared with [^{18}F]FDG PET between patients according to seizure frequency. As shown in Figure 2, data suggest that the intensity of [^{18}F]DPA-714 PET tracer uptake is greater for patients with higher seizure frequency ($p = 0.049$, uncorrected). We did not find any effect of the delay between the [^{18}F]DPA-714 PET and the last seizure on the intensity of the anomalies. We did not find any relationship between the intensity of the anomalies and the age of onset, the duration of the epilepsy, or the presence of frequent focal-to-bilateral seizures.

Region-of-Interest Analysis and AIs

The ROI analysis was more often contributive (ROI value above the limits of the 95% CI of the controls) for [^{18}F]DPA-714 PET (17 or 73.9%) than for [^{18}F]FDG PET (6 or 26.1%) ($p = 0.005$, uncorrected). For 5 patients, ROI analysis was not contributive. Among the 6 patients with contributive [^{18}F]FDG analysis, 5 patients had abnormal values in ROIs consistent with the hypothesis on the location of the EZ. In 2 cases, abnormal values were located in other unrelated ROIs.

Table 1 Characteristics of the Patients Included in the Analysis

Patient	Gender	Age at epilepsy onset (y)	Disease duration (y)	Seizures frequency	Scalp EEG interictal spikes	Ictal video EEG	Langage location	MRI in the suspected EZ	[^{18}F]FDG-PET (hypometabolism)	Phase 1 hypothesis on the EZ	Last seizure before [^{18}F] DPA-714 PET	Age at [^{18}F]DPA-714 PET (y)	Result of blinded [^{18}F] DPA-714 PET analysis	Type of SEEG implantation	Result of SEEG recording	Surgery
1	F	6 mo	19	Monthly	Left FT and bi F	(1) tachycardia with no EEG modification (2) left FT	Left	Left HS	Left T (HC and neocortex) and FB	Left T I F	5 d	19	Left T and I	Left T; I; FB	2 independent L foci (1) 1 subcontinuous mesio T (2) ant I	Left lobectomy T anterior to reduce the most frequent seizures (1)
2	M	12	37	Monthly	Left FT	No focal start	Left	Left parietal DNET	Focal on the MRI lesion	Left P	NA	49	Right TP	Left P T	Extent network overpassing the lesion	Lesionectomy with adjacent cortex
3	M	21	12	Weekly	Left F	Left FT	Left	N	N	Left F	1 d	33	Left I	Left F	1 focus F anterior	No (refused)
4	M	10	23	Weekly	Bi-O	Bioccipital right > left and bi P, and bi central propagation	Left	Right occipital dysplasia	All right hemisphere	Right O	1 d	33	Right O, right amyg, right I opercular	No: functional risk	No: functional risk	No: functional risk
5	F	32	12	Monthly	Right and left T and bi F	Right T with a fast left T propagation	Left	N	Bi-T left > right	Right and left T + right I	8 d	44	Bi HC right > left and bi I	Bi T and bi I and bi F	1 focus mesio T	Right lobectomy T anterior
6	M	33	2	Weekly	2 foci (1) left T (2) right T basal	Right T with fast left T propagation	Left	N	P and bi-T left > right	Right and left T	2 d	35	Left HC and pole and I, focal right cingulum	No (refused)		
7	F	5	14	Monthly	(1) Right FT spikes (2) diffuse slow waves	Right I; ant opercule	Left	N	N	Right I	12 h	19	Right HC right I	Right I T C	1 focus I ant	Right anterior insula
8	F	14	15	Monthly	Diffuse and bi lateral spikes	Left TP	Left	Left paraventricular heterotopia	N	Left P	NA	39	Left post I, left parietal, left HC	Left T P I	No clear focus but heterotopia thermocoagulation	Seizure stop years after heterotopia thermocoagulation
9	M	3	32	Daily	Right T anterior and mild T	(1) Right TO (2) right central	Left	Right occipital dysplasia	Right O and T	Right O	6 h	35	Right O, right I	Right O P T	3 foci (1) O (2) T (3) F	Rejected: multifocal
10	F	18	1	Monthly	Bi T	Right posterior I	Right	Right P meningioangiomatosis	On the lesion and right T pole	Right P	6 h	19	Right P	No (refused)		
11	M	6	23	Daily	Bi T	Left posterior I	Bilat	N	N	Left I T and P	12 h	29	Left I and opercule	Left T P I	1 focus I posterior	Improved by thermocoagulation: if worsening
12	F	29	3	Monthly	Left T anterior and posterior	Left T basal	Bilat R > L	Left abnormal temporo-basal sulcus	Left T basal and T pole	Left T	17 d	32	Left T basal, left T pole, left I post	Left T O	1 focus T basal	Left lobectomy T anterior
13	M	19	16	Monthly	Left T anterior	Left T	Left	N	N	Left T	4 d	35	Left HC and perisylvian area	No (refused)		
14	M	17	13	Monthly	Left T anterior and basal	Left T anterior and bi F	Left	Left temporal anterior meningocele	Left T pole	Left T	6 d	30	All the left T cortex	No (refused)		

Continued

Table 1 Characteristics of the Patients Included in the Analysis *(continued)*

Patient	Gender	Age at epilepsy onset (y)	Disease duration (y)	Seizures frequency	Scalp EEG interictal spikes	Ictal video EEG	Langage location	MRI in the suspected EZ	[^{18}F]FDG-PET (hypometabolism)	Phase 1 hypothesis on the EZ	Last seizure before [^{18}F] DPA-714 PET	Age at [^{18}F]DPA-714 PET (y)	Result of blinded [^{18}F] DPA-714 PET analysis	Type of SEEG implantation	Result of SEEG recording	Surgery
15	M	49	4	Monthly	Left T anterior	Left T basal	Bilat	N	Left T mesial and neocortical	Left T	6 d	53	Left orbitofrontal, I and T	Bi T and left I and F	2 foci (1) left T neocortical (2) I	Left T cortectomy to reduce type 1 seizure frequency
16	M	11	7	Monthly	Left T anterior, T basal or bi F	Left T basal and post I and P	Left	Gyri abnormalities maximal in left P and T basal lobes	N	Left T P I	4 d	18	Left parieto-opercula	Bi T	1 focus left TP region (close to langage area)	Rejected: improved by thermocoagulation; functional risk (langage)
17	M	16	19	Monthly	Right T and P	No focal start: right posterior perisylvian	Left	N	N	Right P	1 d	35	Bi I right > left	Right T, I	1 focus post and inf I	Improved by thermocoag: if worsening
18	F	13	6	Monthly	No	Right T neocortical	Right	N	Slight right T pole	Right T	1 d	29	Right T and HC	Right T, I	No seizure recorded but hematoma on the suspected EZ	Rejected: no more seizures
19	M	11	20	Weekly	Bi F and bi C	Right insula and opercule	Left	N	N	Right I	12 h	31	Right F, I and perisylvian post and left I and opercular	Right F-orbitaire, I, amygdala and left I	1 focus right F-basal and I anterior	To be done
20	F	27	2	Weekly	Left T	Left T ant and basal	Left	N	Left T pole	Left T	4 d	29	Right I and opercular	Rejected: no more seizures		
21	F	9	8	Daily	Bi C left > right	Bi central right > left	Left	N	N	Right F	12 h	17	Focal R precentral	Right F and perirolandic	1 fucus right F on F2 (on motor area)	Functional risk
22	F	18	4	Daily	Bi C	Bi central right > left	Left	N	N	Right F	1 d	21	extent bicentral	Right perirolandic	No focal onset	Rejected: no focal and functional risk
23	F	13	10	Daily	Bi C	Bi central left > right	Left	N	Left T pole	Left C	6 h	16	Left C	No: functional risk	No: functional risk	No: functional risk

Abbreviations: B = basal; C = central; DNET = dysembryoplastic neuroepithelial tumor; EZ = epileptogenic zone; F = female; F = frontal; HC = hippocampus; HS = hippocampal sclerosis; I = insula(r); M = male; N = normal; O = occipital; P = parietal; T = temporal.

Table 2 Comparison of the Visual Analysis of [^{18}F]FDG and [^{18}F]DPA-714 PET of the 23 Patients

	[^{18}F]FDG PET (n = 23)	[^{18}F]DPA-714 PET (n = 23)	*p* Value[a]	Corrected *p* value[b]
Sensitivity				
Presence of an anomaly (yes)	13 (56.5)	22 (95.7)	0.016[c]	0.022[c]
Intensity of anomaly			0.016[c]	0.022[c]
None	10 (43.5)	1 (4.3)		
Mild	6 (30.4)	8 (34.8)		
Intense	7 (26.1)	14 (60.9)		
Accuracy				
Anomaly localization matching the hypothesis on the EZ			0.177	0.177
No	11 (47.8)	4 (17.4)		
Partially	5 (21.7)	4 (17.4)		
Totally	7 (30.4)	15 (65.2)		
Anomaly localization providing new information to refine the EZ hypothesis (yes)	4 (17.4)	15 (65.2)	0.005[c]	0.019[c]
[^{18}F]FDG PET anomaly not detected on [^{18}F]DPA-714 PET (yes)	4 (17.4)			
[^{18}F]DPA-714 PET anomaly not detected on [^{18}F]FDG PET (yes)		21 (91.3)		
Nonrelevant binding on [^{18}F]DPA-714 PET				
Hindering interpretation		4 (17.4)		
Not interfering with interpretation		10 (43.5)		

Abbreviations: DPA = [N,N-diethyl-2-(2-(4-(2[^{18}F]-fluoroethoxy)phenyl)5,7dimethylpyrazolo [1,5a]pyrimidin-3-yl)acétamide; EZ = epileptogenic zone; FDG = fluoro-deoxyglucose.
Data are given as count (percentages) for categorical variables.
[a] Mc-Nemar test was used to compare groups for nonordinal categorical variables and Wilcoxon signed-rank tests for the ordinal categorical variables.
[b] *p* values corrected for multiple testing using Benjamini-Hochberg method.
[c] Statistically significant.

In the 17 patients with contributive [^{18}F]DPA-714 analysis, 15 patients had abnormal values in ROIs consistent with the hypothesis on the EZ localization, and in 9 cases, abnormal values were located in other unrelated ROIs. In the 17 patients with noncontributive [^{18}F]FDG ROI analysis, 12 had a contributive [^{18}F]DPA-714 PET analysis, 11 of which in ROIs consistent with the suspected EZ.

No statistical difference was found between the 2 PET images concerning the lateralizing values of AI: the AI showed PET anomaly ipsilateral to the suspected EZ for 14 (60.9%) patients with [^{18}F]FDG and for 16 patients (69.6%) with [^{18}F]DPA-714, contralateral to the EZ for 4 (17.4%) patients with [^{18}F]FDG and for 1 patient (4.3%) with [^{18}F]DPA-714, and was not contributive (AI value included in the 95% CI of control's AI) for 5 (21.7%) patients with [^{18}F]FDG and for 6 (26.1%) patients with [^{18}F]DPA-714.

Voxel-Wise Analysis

As presented in Table 3 and Figure 1, the voxel-wise analysis of [^{18}F]DPA-714 PET was more likely than [^{18}F]FDG PET to find significant clusters (93.3% vs 52.2%, $p = 0.022$) and was also more likely to show clusters whose localization was consistent with the EZ hypothesis (87.0% vs 39.1%, $p = 0.019$). The clusters with decreased [^{18}F]DPA-714 uptake did not correspond to any particular anatomical distribution or possible pathways of seizure propagation.

This study provides Class IV evidence on the utility of [^{18}F]DPA-714 PET compared with [^{18}F]DPA-714 PET in identifying the epileptic zone in patients undergoing phase 1 presurgical evaluation for intractable epilepsy.

Discussion

In this original study, we compared the performance of [^{18}F]DPA-714 PET with [^{18}F]FDG PET in clinical use conditions. We focused on a population of patients with complex DRFE, in whom the first-line presurgical assessment did not enable a straightforward surgical resection.[31] We were able to show that [^{18}F]DPA-714 is useful in these patients, especially when the [^{18}F]FDG PET is not contributive: [^{18}F]DPA-714 PET shows

Figure 1 Additional Value of [^{18}F]DPA-714 PET to Help Localize the EZ

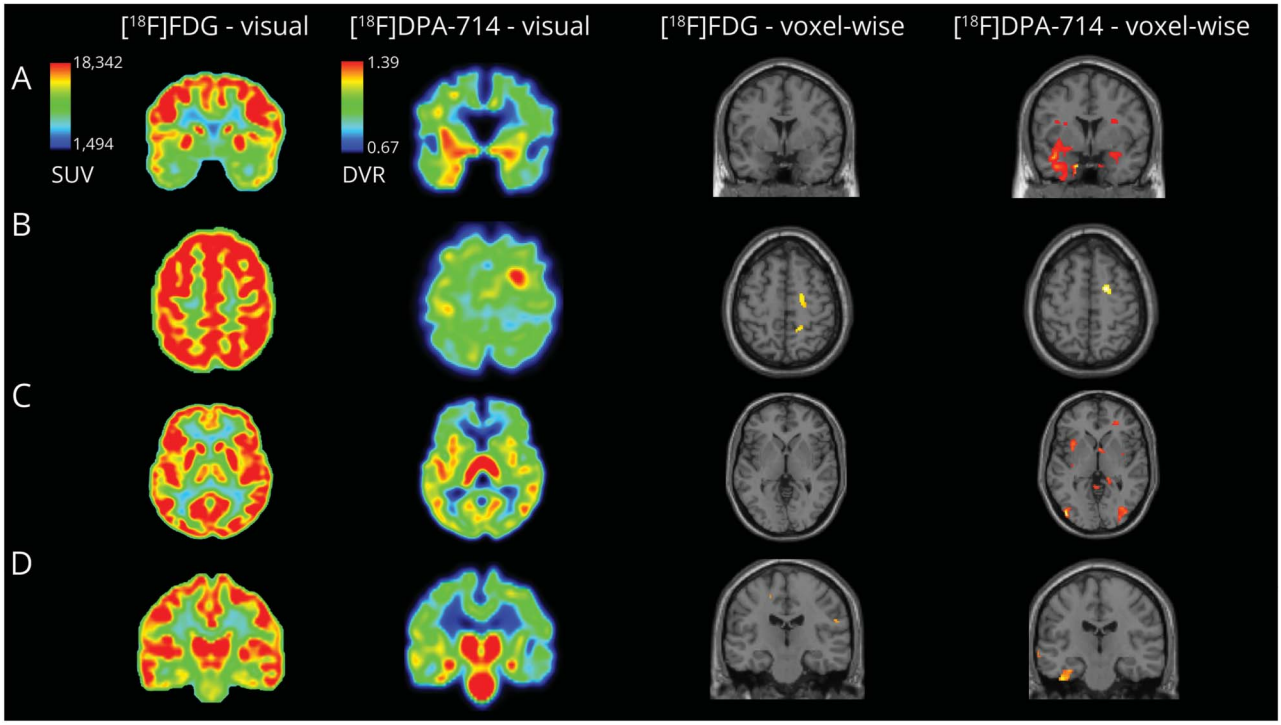

Images shown in anatomical orientation and brain masked, voxel-wise analysis displayed with a $p < 0.005$, k = 50, uncorrected (brain only), in SPM12, overlaid on a standard MRI section illustrating the decrease of [^{18}F]FDG uptake and increase of [^{18}F]DPA-714 in patient compared with control database. Panel A: The patient with a bitemporal suspected EZ. Visual analysis of [^{18}F]FDG PET shows a bitemporal hypometabolism; the left predominance is not clear. Visual analysis of [^{18}F]DPA-714 PET shows a bitemporal increase of the tracer uptake with a strong left predominance. Voxel-wise analysis of the patient's [^{18}F]FDG PET compared with controls' PET does not identify a statistically significant cluster, whereas [^{18}F]DPA-714 PET voxel-wise analysis identifies a large cluster located in the left temporal gray matter and a smaller one in the right hippocampus. Panel B: The patient with a right pericentral suspected EZ. [^{18}F]DPA-714 PET shows a strong and easily noticeable focal uptake increase within the right precentral area. On retrospective analysis of [^{18}F]FDG PET, a sulcal hypometabolism can be seen within the region pointed by [^{18}F]DPA-714 PET. Voxel-wise analysis of the patient's [^{18}F]FDG and [^{18}F]DPA-714 PET compared with controls' PET identify a statistically significant cluster within the right precentral area. Panel C: The patient with a left insulo-parietal suspected EZ. [^{18}F]FDG PET was initially interpreted as normal. On closer inspection, a slight hypometabolism can be seen within the lesion pointed by [^{18}F]DPA-714 PET. [^{18}F]DPA-714 PET shows an increase in tracer uptake within the left anterior and posterior insula. Voxel-wise analysis of the patient's [^{18}F]FDG PET compared with controls' PET does not identify a statistically significant cluster, whereas [^{18}F]DPA-714 PET voxel-wise analysis identifies a cluster located in the anterior insular gray matter. These images also illustrate the presence of nonrelevant fixation in [^{18}F]DPA-714 PET imaging. Panel D: The patient with a left temporal suspected EZ. Visual analysis of [^{18}F]FDG PET shows a bihippocampal hypometabolism, with a left predominance. Visual analysis of [^{18}F]DPA-714 PET shows an increase of the tracer uptake in both hippocampus with a left predominance and in the left collateral sulcus. Voxel-wise analysis of the patient's [^{18}F]FDG PET compared with controls' PET identifies small cluster in the white matter, whereas [^{18}F]DPA-714 PET voxel-wise analysis identifies a large cluster located in the left collateral sulcus. [^{18}F]DPA-714 = [N,N-diethyl-2-(2-(4-(2[^{18}F]-fluoroethoxy)phenyl)5,7dimethylpyrazolo [1,5a]pyrimidin-3-yl)acetamide; [^{18}F]FDG = [^{18}F]-fluorodeoxyglucose; EZ = epileptogenic zone; SPM = statistical parametric mapping.

significantly more anomalies, which are consistent with the electroclinical hypothesis, and provides more new information, which allows to refine the possible localization of the EZ. Subtle anomalies are better highlighted by [^{18}F]DPA-714 PET compared with [^{18}F]FDG PET, as previously suggested by Butler et al.[14] [^{18}F]DPA-714 PET seems to be even more helpful in patients with more complex presurgical assessment, that is, those with negative brain MRI or neocortical localizations.

To date, very few studies on TSPO PET imaging in epilepsy used it as a clinical tool.[12-14,14,16-18] The pioneer work done by the Bethesda team demonstrated that the uptake of ^{11}C-PBR28, another TSPO radioligand, was increased in the hippocampus ipsilateral to the EZ in MTLE.[12,13] In this specific situation, the sensitivity of [^{18}F]FDG PET is very good, with limited need for alternative diagnostic tools.[6] Subsequent studies focused on patients with neocortical epilepsy, in whom [^{18}F]FDG PET is less efficient,[6] demonstrating that TSPO PET imaging could also be a marker of the EZ in these patients, even in the absence of lesions on brain MRI.[17,18] This study, which included a high proportion of patients with normal MRI (65.2% vs 33%–45% in the other studies), supports these data as TSPO imaging was capable of detecting an anomaly in 100% of patients with normal MRI (55.5% in the study by Kagitani-Shimono et al. and 20% in the study by Dickstein et al.).[17,18] When [^{18}F]FDG PET showed anomalies, the TSPO PET was also consistently positive in helping to lateralize the EZ or highlighting an anomaly in the insular or cingulate cortex.[17,18] In this study, when [^{18}F]FDG PET failed to detect the EZ, TSPO PET was found to be very effective in detecting an anomaly (100% in visual analysis, 70.8% in ROI analysis) (similar results found by Dickstein et al.[17]). Similarly, the strong correspondence between TSPO PET anomalies and the hypothesis on the EZ is similar in this study and in the cohort of Kagitani-Shimono et al. (82.6% vs 81.5%).[18]

Figure 2 [^{18}F]DPA-714 Uptake Increase, Scored in Qualitative Visual Analysis, Seems to Be Greater With Increased Seizure Frequency (p = 0.049)

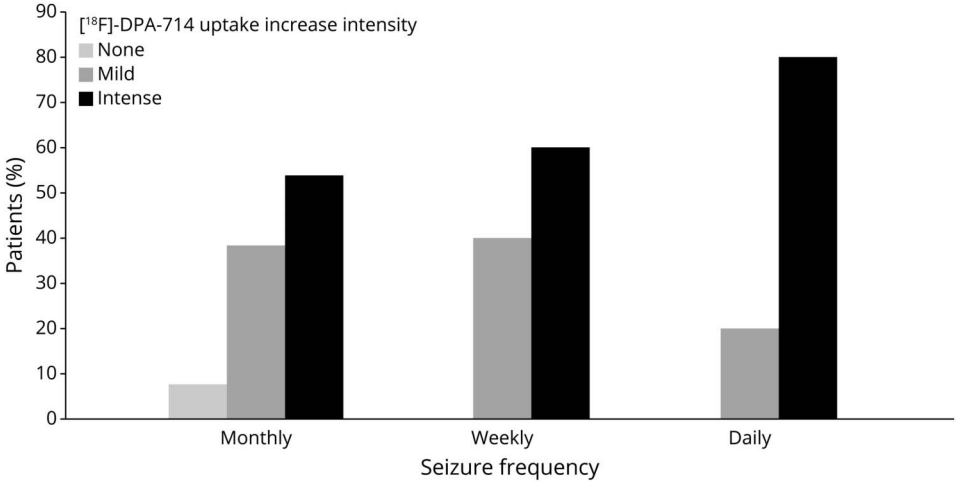

[^{18}F]DPA-714 = [N,N-diethyl-2-(2-(4-(2 [^{18}F]-fluoroethoxy)phenyl)5,7dimethylpyrazolo [1,5a]pyrimidin-3-yl)acetamide.

This work provides interesting results for patients with seizure semiology suggesting an insular involvement,[32] for whom imaging and electrophysiology are often inconclusive.[33] [^{18}F]DPA-714 PET seems to be more effective than [^{18}F]FDG PET in revealing abnormal tracer fixation in the insula of these patients, as previously suggested by the results from Kagitani-Shimono et al.

We did not find association between the delay since the last seizure and the [^{18}F]DPA-714 PET uptake, unlike the results from Butler et al.[15] One possible explanation is that none of the patients underwent PET acquisition after a prolonged seizure-free period, and the differences between the patients on this parameter were too small to highlight any difference (first quartile: 1 day; third quartile: 5.75 days). On the contrary, this study reinforces the preclinical findings in rodents, which suggested a higher fixation of TSPO tracer in individuals with more frequent seizures.[34]

The study population is highly selected, including patients without major cerebral lesions that would make automatic segmentation difficult. This reduces the scope of these results, excluding patients with large lesions (e.g., polymicrogyria, tuberous sclerosis, previously operated patients). The acquisition and postprocessing of [^{18}F]DPA-714 PET images used in this study are not adapted to an easy use in clinical settings. First, the use of the Logan reference plot technique requires dynamic image acquisition over 90 minutes, and second, the algorithm required for the SVCA normalization method is difficult to implement. We decided to use these techniques because the use of an arterial input function was not applicable in clinical settings.[26,27,35] Under these conditions, the combination of the Logan plot technique and the SVCA method, previously demonstrated to give equivalent results to an arterial input function,[26,36] was the most appropriate analytic method.

The use of a PET/MR system for [^{18}F]DPA-714 PET (whereas [^{18}F]FDG PET was acquired on a PET/CT) is also a limitation, as different attenuation correction method may introduce a bias in the semiquantitative values. However, we focused on the differences between the signal of healthy and pathologic regions of an individual (not the raw values) so that if such a bias exists, it will not affect the results.

Another weakness of TSPO PET imaging is the areas of increased tracer uptake, referred to as nonrelevant when the interpretation is guided by clinical data. It can be found, in healthy controls and patients, in the brainstem and thalamus.[13] This prompted the use of a mask excluding the brainstem and the extracerebral tissues in this study. As previously reported, nonrelevant increase in tracer uptake can be located in choroid plexus affecting the temporal lobe signal.[12,13,37] However, these nonrelevant binding may also differ between individuals, affecting cortical gray matter.[17] We found these nonrelevant binding in 14 of 23 patients (60.8%) in visual analysis, including 4 cases (17.4%) where they interfered with the interpretation of the images, and in 9 patients of 23 in voxel-wise analysis (compared with 2 patients for the [^{18}F]FDG PET). The higher number of controls in future studies could limit this bias in quantitative analyses. This highlights the importance of image analysis being guided by electroclinical data, as recommended by the ILAE.[2,38]

Although the subjectivity of the qualitative visual approach can be criticized, it seemed to be the most sensitive method in this study. The very good interobserver agreement demonstrated the minimal impact of this bias. If quantitative voxel-wise or ROI analysis may seem attractive, these results show that their findings did not significantly help to localize the EZ, either with [^{18}F]FDG or [^{18}F]DPA-714 PET. The ROI approach is often used in PET imaging. In epilepsy imaging, it seems less relevant because PET anomalies may overlap several ROIs or may be very limited in size (in such situations, the mean value of the

Table 3 Comparison of the Voxel-Wise Analysis of [^{18}F]FDG and [^{18}F]DPA-714 PET of the 23 Patients

	[^{18}F]FDG PET (n = 23)	[^{18}F]DPA-714 PET (n = 23)	*p* Value[a]	Corrected *p* value[b]
Sensitivity				
Presence of a significant cluster (yes)	12 (52.2)	21 (91.3)	0.0158[c]	0.022[c]
Principal cluster extend[d,e] (voxel)	147.0 [88.5; 478.5]	199.0 [125.0; 586.0]	0.577	
Principal cluster *p* value[d,e]	0.014 [0.000; 0.098]	0.000 [0.000; 0.000]	0.014[c]	
Accuracy				
Cluster[d] localization matching the EZ hypothesis (yes)	9 (39.1)	20 (87.0)	0.005[c]	0.019[c]
Cluster[d] localization providing new information on the EZ (yes)	4 (17.4)	11 (47.8)	0.070	0.082
[^{18}F]FDG PET cluster not detected on [^{18}F]DPA-714 PET (yes)	5 (21.7)			
[^{18}F]DPA-714 PET cluster not detected on [^{18}F]FDG PET (yes)		17 (73.9)		

Abbreviations: DPA = [N,N-diethyl-2-(2-(4-(2[^{18}F]-fluoroethoxy)phenyl)5,7dimethylpyrazolo [1,5a]pyrimidin-3-yl)acétamide; EZ = epileptogenic zone; FDG = fluoro-deoxyglucose; SEEG = stereo-EEG.
Data are given as count (percentages) for categorical variables and as median [Q1; Q3] for numerical variables.
[a] McNemar test was used to compare groups for categorical variables.
[b] *p* Values corrected for multiple testing using Benjamini-Hochberg method.
[c] Statistically significant.
[d] Cluster that was the larger and with the smallest *p* value was selected.
[e] *p* values were not included in the correction for multiple testing due to the exploratory purpose.

ROI is not affected). The AI was widely used in previous work on TSPO imaging.[12,17,18] However, in the case of bilateral anomaly without side predominance, the AI is normal which may be misleading (leading to conclude either to a bilateral epileptogenicity or an absence of fixation in these regions). Moreover ROI analysis is constraint by anatomical features (surface uptake and delineation). Alternatively, voxel-wise analysis does not rely on any kind of anatomical constraint, but it suffered from a lack of power due to the individual vs group analysis design required in epilepsy (as each patient is unique). In addition, we had a small number of controls (n = 11) in [^{18}F]DPA-714 which may have limited the sensitivity of this analysis. Figure 1 illustrates the rare cases where the voxel-wise analysis was efficient.

Both of these semiquantitative approaches are limited by unresolved issues in [^{18}F]DPA-714 PET quantification.[8,19,35] Beyond the issue of the influence of rs6971 polymorphism, other considerations make the use of TSPO ligands complex. Because of the constitutive expression of TSPO in vascular endothelial cells and the ubiquitous distribution of vessels in the brain, it is impossible to define a reference region that is completely free of tracer binding.[9] This may lead to a decrease in TSPO imaging sensitivity. The question of the most appropriate "pseudoreference" region for TSPO PET kinetic modeling is still a matter of discussion in the literature.[19,35,39]

This study provides preliminary evidence that [^{18}F]DPA-714 PET imaging could provide valuable additional value to the presurgical assessment of patients with drug-resistant focal epilepsy and could become an additional tool to help to the localization of the EZ, especially in patients with negative [^{18}F]FDG PET, normal MRI, or neocortical epilepsy, especially insular epilepsy. However, these are only exploratory results that will require further evaluation. [^{18}F]DPA-714 PET seems to be more sensitive than [^{18}F]FDG PET, more often consistent with electrophysiologic and seizure semiology data, and to provide additional information on the cortical areas involved in the EZ. [^{18}F]DPA-714 PET could overcome the limitations of [^{18}F]FDG imaging and thereby add accuracy to the phase 1 presurgical assessment or even prevent invasive intracerebral exploration in borderline cases. Further comparison of [^{18}F]DPA-714 PET with the "gold standard" for the localization of the EZ, that is., intracerebral EEG recording and postoperative outcomes, could enable a better understanding of the accuracy of [^{18}F]DPA-714 PET for the EZ localization.

Acknowledgment

M. Cheval acknowledges the Société Française de Neurologie for their research grant. This work was performed on a platform funded by the France Life Imaging network (Grant No. ANR-11-INBS-0006). The authors thank all the SHFJ team for their help.

Study Funding

This study was funded by the French Federation for Epilepsy Research (FFRE) and a research grant (M. Cheval) from the French Neurology Society (Société Française de Neurologie).

Disclosure

The authors report no relevant disclosures. Go to Neurology.org/N for full disclosures.

Publication History

Received by *Neurology* June 7, 2023. Accepted in final form July 17, 2023. Submitted and externally peer reviewed. The handling editor was Associate Editor Barbara Jobst, MD, PhD, FAAN.

Appendix Authors

Name	Location	Contribution
Margaux Cheval, MD	Université Paris-Saclay, France	Drafting/revision of the manuscript for content, including medical writing for content; major role in the acquisition of data; study concept or design; analysis or interpretation of data
Sebastian Rodrigo, MD, PhD	BioMAPS, Paris, France	Drafting/revision of the manuscript for content, including medical writing for content; major role in the acquisition of data; analysis or interpretation of data
Delphine Taussig, MD, PhD	Bicetre University Hospital, Paris, France	Drafting/revision of the manuscript for content, including medical writing for content; major role in the acquisition of data
Fabien Caillé, PhD	BioMAPS, Paris, France	Major role in the acquisition of data
Ana Maria Petrescu, MD	Bicetre University Hospital, Paris, France	Major role in the acquisition of data
Michel Bottlaender, MD	Université Paris-Saclay, France	Drafting/revision of the manuscript for content, including medical writing for content; major role in the acquisition of data
Nicolas Tournier, PharmD, PhD	Université Paris-Saclay, France	Major role in the acquisition of data
Florent L. Besson, MD, PhD	BioMAPS, Paris, France	Drafting/revision of the manuscript for content, including medical writing for content; major role in the acquisition of data
Claire Leroy, PhD	Université Paris-Saclay, France	Drafting/revision of the manuscript for content, including medical writing for content; major role in the acquisition of data; analysis or interpretation of data
Viviane Bouilleret, MD, PhD	Imagerie Moléculaire In Vivo, SHFJ, CEA, Orsay, France	Drafting/revision of the manuscript for content, including medical writing for content; major role in the acquisition of data; study concept or design; analysis or interpretation of data

References

1. Kwan P, Schachter SC, Brodie MJ. Drug-resistant epilepsy. *N Engl J Med*. 2011;365(10):919-926. doi:10.1056/nejmra1004418
2. Neuroimaging Subcommision of the International League Against Epilepsy. Commission on diagnostic strategies: recommendations for functional neuroimaging of persons with epilepsy. *Epilepsia*. 2000;41(10):1350-1356. doi:10.1111/j.1528-1157.2000.tb04617.x
3. Guidelines for neuroimaging evaluation of patients with uncontrolled epilepsy considered for surgery. Commission on Neuroimaging of the International League Against Epilepsy. *Epilepsia*. 1998;39(12):1375-1376. doi:10.1111/j.1528-1157.1998.tb01341.x
4. Wong CH, Bleasel A, Wen L, et al. Relationship between preoperative hypometabolism and surgical outcome in neocortical epilepsy surgery. *Epilepsia*. 2012;53(8):1333-1340. doi:10.1111/j.1528-1167.2012.03547.x
5. Chassoux F, Rodrigo S, Semah F, et al. FDG-PET improves surgical outcome in negative MRI Taylor-type focal cortical dysplasias. *Neurology*. 2010;75(24):2168-2175. doi:10.1212/wnl.0b013e31820203a9
6. Steinbrenner M, Duncan JS, Dickson J, et al. Utility of 18F-fluorodeoxyglucose positron emission tomography in presurgical evaluation of patients with epilepsy: a multicenter study. *Epilepsia*. 2022;63(5):1238-1252. doi:10.1111/epi.17194
7. Theodore WH, Sato S, Kufta C, Balish MB, Bromfield EB, Leiderman DB. Temporal lobectomy for uncontrolled seizures: the role of positron emission tomography. *Ann Neurol*. 1992;32(6):789-794. doi:10.1002/ana.410320613
8. Bouilleret V, Dedeurwaerdere S. What value can TSPO PET bring for epilepsy treatment? *Eur J Nucl Med Mol Imaging*. 2021;49(1):221-233. doi:10.1007/s00259-021-05449-2
9. Nutma E, Ceyzériat K, Amor S, et al. Cellular sources of TSPO expression in healthy and diseased brain. *Eur J Nucl Med Mol Imaging*. 2021;49(1):146-163. doi:10.1007/s00259-020-05166-2
10. James ML, Fulton RR, Vercoullie J, et al. DPA-714, a new translocator protein-specific ligand: synthesis, radiofluorination, and pharmacologic characterization. *J Nucl Med*. 2008;49(5):814-822. doi:10.2967/jnumed.107.046151
11. Chauveau F, Van Camp N, Dollé F, et al. Comparative evaluation of the translocator protein radioligands 11C-DPA-713, 18F-DPA-714, and 11C-PK11195 in a rat model of acute neuroinflammation. *J Nucl Med*. 2009;50(3):468-476. doi:10.2967/jnumed.108.058669
12. Hirvonen J, Kreisl WC, Fujita M, et al. Increased in vivo expression of an inflammatory marker in temporal lobe epilepsy. *J Nucl Med*. 2012;53(2):234-240. doi:10.2967/jnumed.111.091694
13. Gershen LD, Zanotti-Fregonara P, Dustin IH, et al. Neuroinflammation in temporal lobe epilepsy measured using positron emission tomographic imaging of translocator protein. *JAMA Neurol*. 2015;72(8):882-888. doi:10.1001/jamaneurol.2015.0941
14. Butler T, Ichise M, Teich AF, et al. Imaging inflammation in a patient with epilepsy due to focal cortical dysplasia. *J Neuroimaging*. 2013;23(1):129-131. doi:10.1111/j.1552-6569.2010.00572.x
15. Butler T, Li Y, Tsui W, et al. Transient and chronic seizure-induced inflammation in human focal epilepsy. *Epilepsia*. 2016;57(9):e191-e194. doi:10.1111/epi.13457
16. Banati RB, Goerres GW, Myers R, et al. [11C](R)-PK11195 positron emission tomography imaging of activated microglia in vivo in Rasmussen's encephalitis. *Neurology*. 1999;53(9):2199-2203. doi:10.1212/wnl.53.9.2199
17. Dickstein LP, Liow J, Austermuehle A, et al. Neuroinflammation in neocortical epilepsy measured by PET imaging of translocator protein. *Epilepsia*. 2019;60(6):1248-1254. doi:10.1111/epi.15967
18. Kagitani-Shimono K, Kato H, Kuwayama R, et al. Clinical evaluation of neuroinflammation in child-onset focal epilepsy: a translocator protein PET study. *J Neuroinflammation*. 2021;18(1):8. doi:10.1186/s12974-020-02055-1
19. Scott G, Mahmud M, Owen DR, Johnson MR. Microglial positron emission tomography (PET) imaging in epilepsy: applications, opportunities and pitfalls. *Seizure*. 2017;44:42-47. doi:10.1016/j.seizure.2016.10.023
20. Owen DR, Yeo AJ, Gunn RN, et al. An 18-kDa translocator protein (TSPO) polymorphism explains differences in binding affinity of the PET radioligand PBR28. *J Cereb Blood Flow Metab*. 2012;32:1-5. doi:10.1038/jcbfm.2011.147
21. Lavisse S, Goutal S, Wimberley C, et al. Increased microglial activation in patients with Parkinson disease using [18F]-DPA714 TSPO PET imaging. *Parkinsonism Relat Disord*. 2021;82:29-36. doi:10.1016/j.parkreldis.2020.11.011
22. Hamelin L, Lagarde J, Dorothée G, et al. Early and protective microglial activation in Alzheimer's disease: a prospective study using 18F-DPA-714 PET imaging. *Brain*. 2016;139(4):1252-1264. doi:10.1093/brain/aww017
23. Hamelin L, Lagarde J, Dorothée G, et al. Distinct dynamic profiles of microglial activation are associated with progression of Alzheimer's disease. *Brain*. 2018;141(6):1855-1870. doi:10.1093/brain/awy079
24. Chassoux F, Semah F, Bouilleret V, et al. Metabolic changes and electro-clinical patterns in mesio-temporal lobe epilepsy: a correlative study. *Brain*. 2004;127(1):164-174. doi:10.1093/brain/awh014
25. Sekine T, ter Voert EE, Warnock G, et al. Clinical evaluation of zero-echo-time attenuation correction for brain 18F-FDG PET/MRI: comparison with atlas attenuation correction. *J Nucl Med*. 2016;57(12):1927-1932. doi:10.2967/jnumed.116.175398
26. García-Lorenzo D, Lavisse S, Leroy C, et al. Validation of an automatic reference region extraction for the quantification of [18F]DPA-714 in dynamic brain PET studies. *J Cereb Blood Flow Metab*. 2018;38(2):333-346. doi:10.1177/0271678x17692599
27. Schubert J, Tonietto M, Turkheimer F, Zanotti-Fregonara P, Veronese M. Supervised clustering for TSPO PET imaging. *Eur J Nucl Med Mol Imaging*. 2021;49(1):257-268. doi:10.1007/s00259-021-05309-z
28. Boellaard R, Turkheimer FE, Hinz R, et al. Performance of a modified supervised cluster algorithm for extracting reference region input functions from (R)-[^{11}C]PK11195 brain PET studies. *2008 IEEE Nucl Sci Symp Conf Rec*. 2008:5400-5402. doi:10.1109/NSSMIC.2008.4774453
29. Logan J, Fowler JS, Volkow ND, Wang GJ, Ding YS, Alexoff DL. Distribution volume ratios without blood sampling from graphical analysis of PET data. *J Cereb Blood Flow Metab*. 1996;16(5):834-840. doi:10.1097/00004647-199609000-00008
30. Hammers A, Allom R, Koepp MJ, et al. Three-dimensional maximum probability atlas of the human brain, with particular reference to the temporal lobe. *Hum Brain Mapp*. 2003;19(4):224-247. doi:10.1002/hbm.10123
31. Zijlmans M, Zweiphenning W, van Klink N. Changing concepts in presurgical assessment for epilepsy surgery. *Nat Rev Neurol*. 2019;15(10):594-606. doi:10.1038/s41582-019-0224-y
32. Singh R, Principe A, Tadel F, et al. Mapping the insula with stereo-electroencephalography: the emergence of semiology in insula lobe seizures. *Ann Neurol*. 2020;88(3):477-488. doi:10.1002/ana.25817

33. Harroud A, Bouthillier A, Weil AG, Nguyen DK. Temporal lobe epilepsy surgery failures: a review. *Epilepsy Res Treat*. 2012;2012:201651. doi:10.1155/2012/201651
34. Dedeurwaerdere S, Callaghan PD, Pham T, et al. PET imaging of brain inflammation during early epileptogenesis in a rat model of temporal lobe epilepsy. *EJNMMI Res*. 2012;2(1):60. doi:10.1186/2191-219x-2-60
35. Wimberley C, Lavisse S, Hillmer A, Hinz R, Turkheimer F, Zanotti-Fregonara P. Kinetic modeling and parameter estimation of TSPO PET imaging in the human brain. *Eur J Nucl Med Mol Imaging*. 2021;49(1):246-256. doi:10.1007/s00259-021-05248-9
36. Lavisse S, García-Lorenzo D, Peyronneau MA, et al. Optimized quantification of translocator protein radioligand ^{18}F-DPA-714 uptake in the brain of genotyped healthy volunteers. *J Nucl Med*. 2015;56(7):1048-1054. doi:10.2967/jnumed.115.156083
37. Ricigliano VAG, Morena E, Colombi A, et al. Choroid plexus enlargement in inflammatory multiple sclerosis: 3.0-T MRI and translocator protein PET evaluation. *Radiology*. 2021;301(1):166-177. doi:10.1148/radiol.2021204426
38. Gaillard WD, Chiron C, Helen Cross J, et al. Guidelines for imaging infants and children with recent-onset epilepsy. *Epilepsia*. 2009;50(9):2147-2153. doi:10.1111/j.1528-1167.2009.02075.x
39. Lyoo CH, Ikawa M, Liow JS, et al. Cerebellum can serve as a pseudo-reference region in Alzheimer disease to detect neuroinflammation measured with PET radioligand binding to translocator protein. *J Nucl Med*. 2015;56(5):701-706. doi:10.2967/jnumed.114.146027